Kovacevic, A., Rane, S. & Stosic, N. (2013). Grid Generation for Screw Compressors with Variable Geometry Rotors. International Journal of Aerospace and Lightweight Structures, 3(2), doi: 10.3850/S2010428613000603

International Journal of Aerospace and Lightweight Structures (IJALS)

GRID GENERATION FOR SCREW COMPRESSORS WITH VARIABLE GEOMETRY ROTORS

AHMED KOVACEVIC*, SHAM RANE and NIKOLA STOSIC

Centre for positive displacement compressor technology, City University London, Northampton Square, London, EC1V 0HB, United Kingdom
a.kovacevic@city.ac.uk

Received 16November2013
Revised Day Month Year

An algebraic grid generation algorithm is presented in this paper which enables the performance of twin screw compressors with variable rotor geometry to be predicted, by means of Computational Fluid Dynamics (CFD). It is based on a method, previously developed by the authors, for compressors with standard uniform pitch rotors and constant cross-section profile, which has now been extended to include rotors with variable pitch and/or variable profile. By its use with the commercial CFD solver ANSYS CFX, it has been possible to obtain performance predictions for three variants of an oil-free 3/5 screw compressor, namely uniform helical rotors, variable pitch rotors and variable profile rotors. The variable pitch and variable profile rotors achieve steeper internal pressure rise and a larger discharge area for the same pressure ratio. Variable pitch rotors also showed lower leakage rates due to reduced sealing line length in the high pressure domain. This grid generating procedure advances the ability to evaluate both existing and novel compressor configurations.

Keywords:Algebraic Grid Generation; Computational Fluid Dynamics; Twin Screw Compressor; Variable Pitch Rotors; Variable Profile Rotors.

1. Introduction

Twin screw compressors contain helically lobed rotors with profiles that optimize the compression process. The pitch of screw compressor rotors is defined as the axial distance between the tips of consecutive lobes. This is normally constant along the rotor length. Fig.1shows a CAD model of a twin screw compressor consisting of the compression chamber formed between the helical rotors and casing. Such a domain includes the main chamber, the leakage paths, and the rotor ports. Rotors with variable pitch were patented by Gardner in 1969 but are rarely used due to the lack of cost effective manufacturing techniques for their production.Fig.2 shows a pair of twin screw rotors with variable pitch. It has been shown in the literature that for the same rotor lengths, diameter, wrap angles and lobe profiles, variable pitch rotors can provide a higher pressure ratio and larger discharge port opening areas than the equivalent rotors of constant pitch with reduced throttling losses [Gardner, 1969]. Even higher compression ratios could be achieved when the rotors are of variable diameter.

*City University London, Tait Building, CG07, School of Engineering and Mathematical Sciences, Northampton Square, EC1V 0HB, London, United Kingdom
tel: +44 20 7040 8780, fax: +44 20 7040 8566.

Twin screw machines are today often analysed by the use of Computational Fluid Dynamics (CFD). The prerequisite for successful CFD analysis is appropriate space discretization by a suitable numerical grid. Three main mathematical methods are used to generate such grids, namely algebraic methods, differential methods and variational methods, as described in Eiseman [1992], Liseikin [1998, 1999], Samareh and Smith [1992], Shih et. al. [1991], Soni [1992] and Thompson [1999]. The use of general purpose grid generators for screw compressors has been found to be inadequate and only customized grid generation programs have been found to be suitable for twin screw compressor applications[Kovacevic et. al., 2007, Prasad, 2004,Voorde et. al., 2004, Rane et. al., 2013].

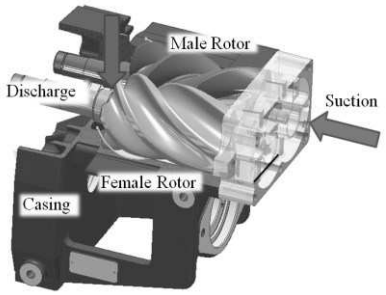

Fig.1.Sectioned view of a Twin Screw Compressor

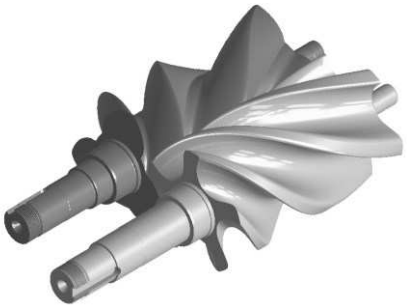

Fig.2. Variable Pitch Screw Rotors

Kovacevic et. al. [2000, 2002, 2004, 2005 and 2007] have successfully used an algebraic grid generation method to produce a numerical mesh for twin screw machines with constant pitch rotors. This has been implemented in a customized program called Screw Compressor Rotor Grid Generator. Fig.3 shows an example of one cross-section in a grid produced by this method.

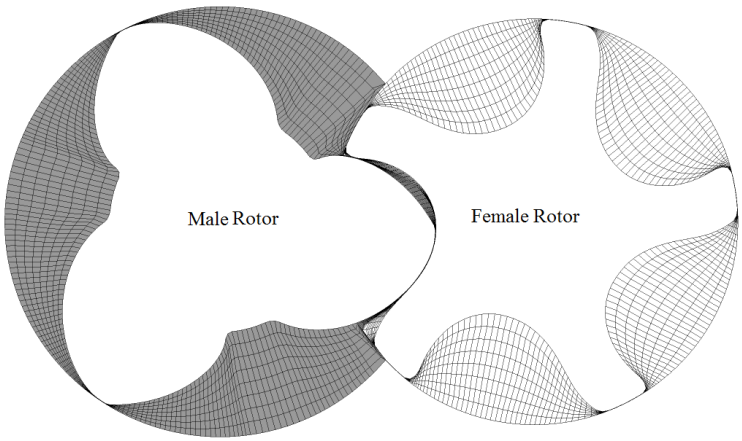

Fig.3. Numerical grid in cross section

2. Grid Generation for variable geometry rotors

Rotors with a uniform pitch and a constant rotor profile have a fixed relationship between the lead and rotor rotation angles. This allows for the numerical grids generated in one cross section at different angular positions in time to be used conveniently for spatial definition of rotors along the rotor axis. The challenge in generating a numerical grid for variable lead rotors is in establishing the relationship of the axial distance between consecutive cross sections and the angular rotation of the rotor. Uniform rotation does not correspond to the uniform axial spacing of cross sections in variable pitch rotors. Fig.4 shows the difference in grid spacing for constant and variable pitch rotors.

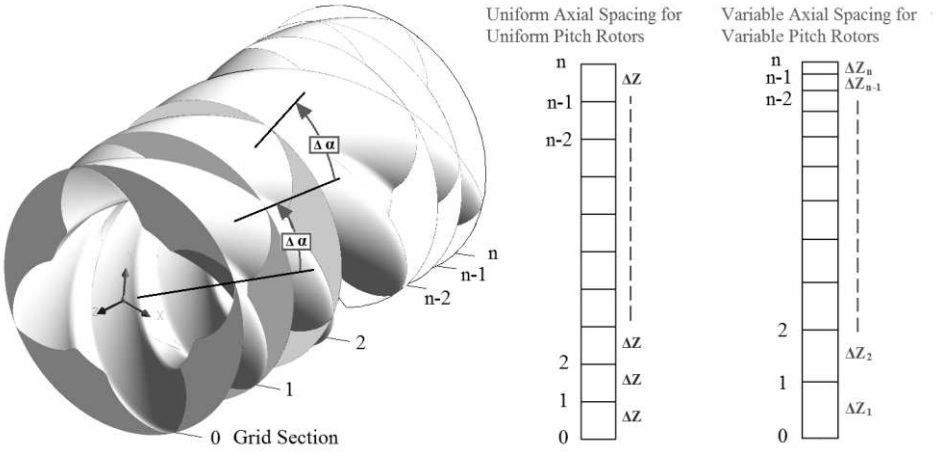

Fig.4. Cross sectional spacing for uniform and variable pitch rotors

The rotor pitch is usually constant. However it can also change linearly, non-linearly or in steps. The former is often used for screw vacuum pumps while the latter is applied in some car superchargers. The change in the pitch can be expressed through following equations:

Constant Pitch

$$p = \text{constant} \tag{2.1}$$

Linear Pitch

$$p = \left(\frac{p_e - p_s}{L}\right) z + p_s \tag{2.2}$$

Quadratic Pitch

$$p = \left(\frac{p_e - p_s}{L^2}\right) z^2 + p_s \tag{2.3}$$

The authors have developed two approaches for grid generation for machines with variable pitch rotors, as described in detail in previous publications [Rane et. al., 2013].
The first approach uses relations like equations (2.1) to (2.3) to define the corresponding axial distance at different axial positions of a cross section ΔZ_n which relate to a uniform rotation of $\Delta\alpha$. It does not allow change of a profile along the rotor axis. The second approach, shown in Fig.5, is more general. Here, it is assumed that screw compressor

rotors form a conjugate pair in each cross section. Therefore each section can be calculated independently using its specific rotor profile.

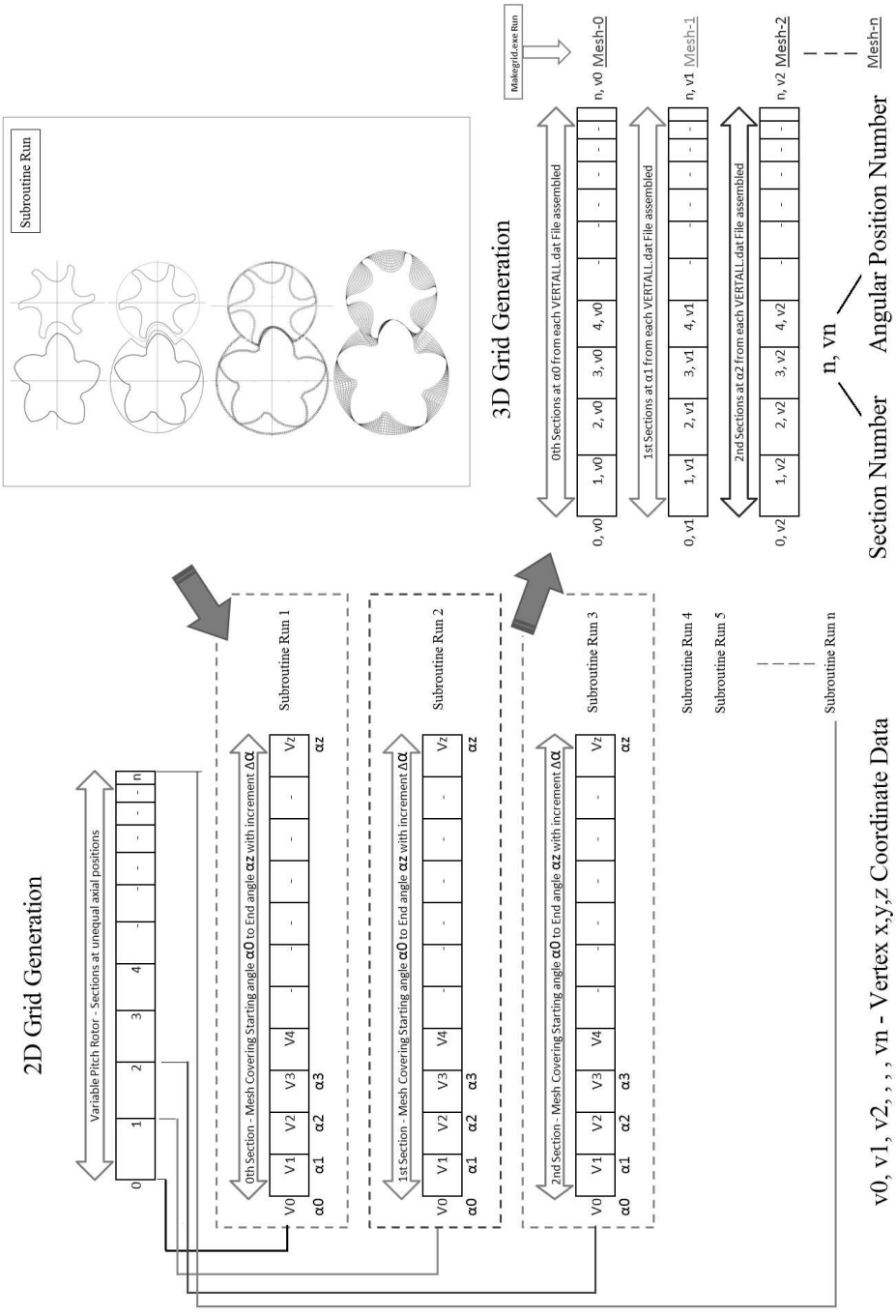

Fig.5. Variable Pitch and Variable Profile Grid Generation

An example of a constant rotor profile with variable pitch rotors is shown in Fig. 7 while the grid for variable rotor geometry and uniform pitch is shown in Fig. 8.

3. CFD Analysis

Numerical analysis was carried out by use of the ANSYS CFX solver in order to validate the grid generation approach for a variable rotor profile and to study the performance of compressors with various configurations. The male rotor had 3 lobes with 127.45mm outer diameter, L/D ratio 1.6 and a wrap angle Φ_w of 285°. The female rotor had 5 lobes and the rotor center distance was 93mm. Both rotors had rack generated 'N' profiles. The compressor speed was 8000 rpm with assumed pressure ratios of 2:1 and 3:1.

3.1. *Case description*

Three test cases were calculated.

Case 1. Uniform pitch and uniform profile rotors with built in volume index V_i of 1.8.

Case 2. Uniform Pitch and Profile rotors with a reduced discharge port opening area to give a built in volume index V_i of 2.2. In this case, the compression chamber is exposed to the discharge pressure relatively late in the cycle as shown in Fig. 6 and allows for further pressure build up in the chambers.

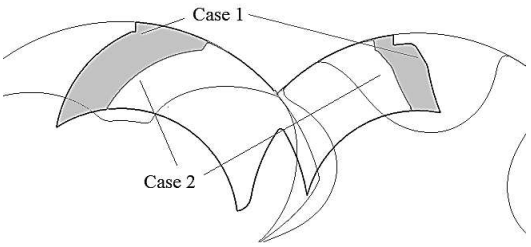

Fig. 6. Reduced discharge port area in Case 2 compared with Case 1

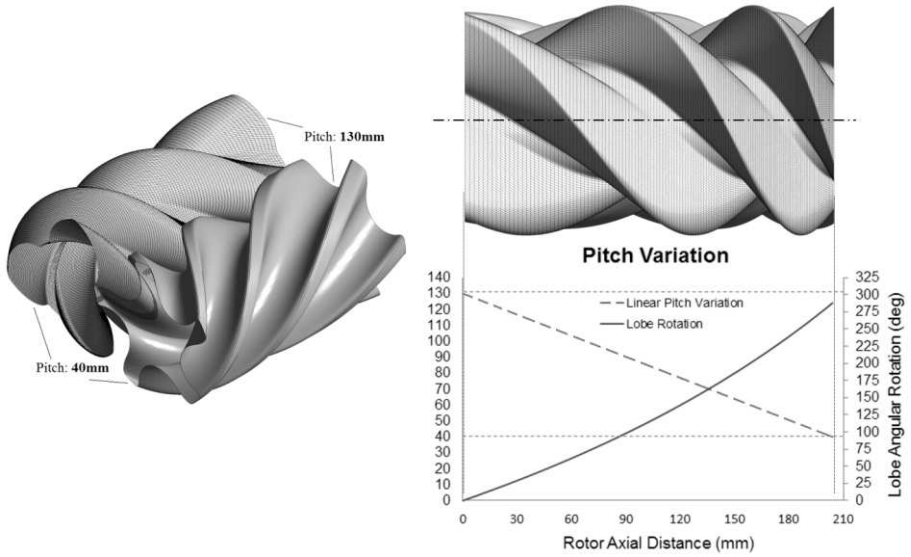

Fig. 7. Variable pitch grid – 3/5 'N' rotors with Case 3

Case 3. Variable pitch with uniform profile rotors and built in volume index $V_i > 1.8$. The Suction side pitch was 130mm and Discharge side pitch was 40mm. The wrap angle of Φ_w 285° was maintained as shown in Fig. 7.

Case 4. Variable profile and uniform pitch rotors. The rotor profile in successive sections was generated using a rack generation procedure by varying the addendum on the defining racks [Stosic, 1998]. The addendum on the suction end of the rotors was 33mm while on the discharge side it was reduced to 21mm. The addendum on the uniform profile rotors had a constant value of 28.848mm. Due to variation of the addendum, the outer diameter of the male rotor changed while the inner diameter remained constant and vice versa for the female rotor as shown in Fig. 8. The volumetric displacement of these rotors is smaller than for uniform profile rotors.

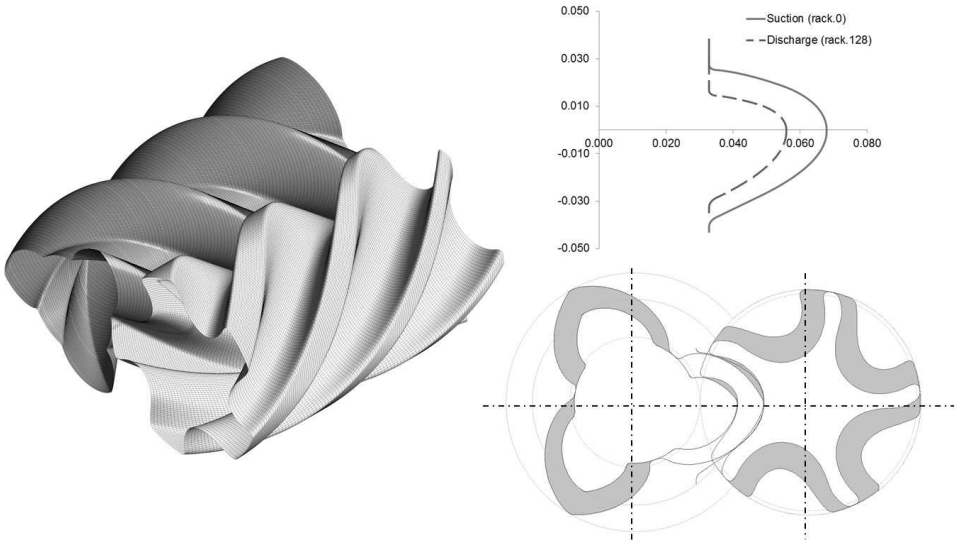

Fig. 8. Variable profile grid – 3/5 'N' rotors with Case 4

3.2. *Simulation description*

Each rotor configuration was analyzed with three levels of successive grid refinements. Table 1 shows the number of computational nodes in each case. The stationary compressor ports were meshed by the use of a commercial grid generator. Fig. 9 shows the different parts of the numerical model and the grid refinement is shown in Fig. 10.

Table 1. Grid refinement shown as number of computational nodes.

Case	Uniform	Variable Pitch	Variable Profile
Coarse	691174	648190	675918
Medium	838378	915184	889794
Fine	1214418	1344944	1297434

The numerical solver used for the study was the ANSYS CFX [2011], which uses a vertex-based Finite Volume Method and solves for momentum and continuity in a pressure coupled algorithm iteratively. All the generated grids are passed to the solver in the model setup and during the solution the rotor domain grids are updated for every time step, by external subroutines. The space conservation law is retained during this grid motion by modification of the governing equation, as described by Ferziger and Peric [1996]. The solver was set with a Higher Order advection scheme and a Second Order Backward Euler temporal discretization.

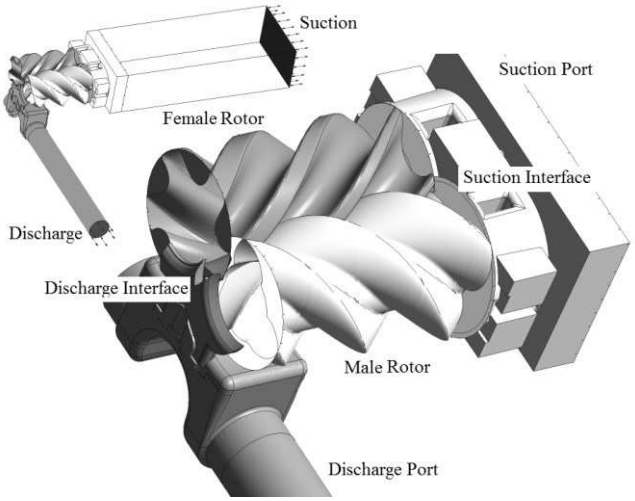

Fig. 9. Twin screw compressor working chamber domains

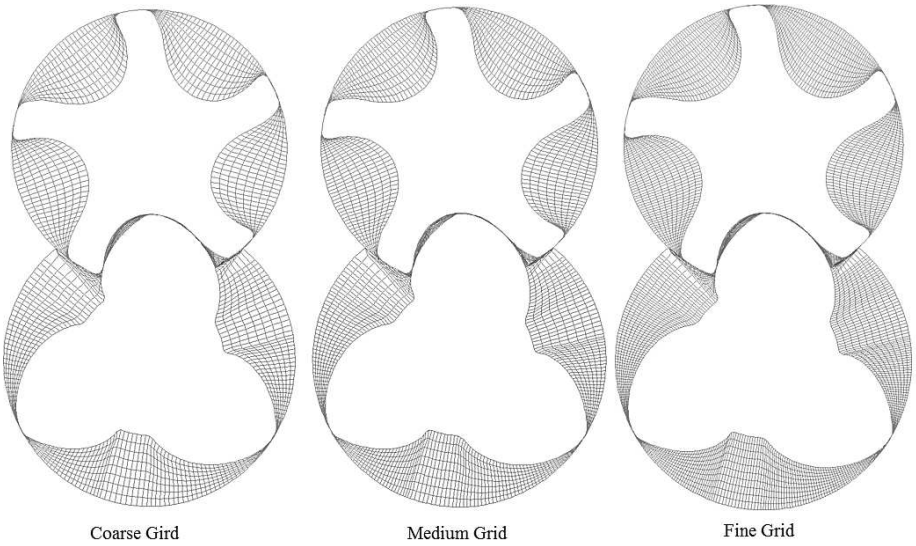

Fig. 10. Different levels of grid refinement shown for one cross section

The tetrahedral meshes of the ports and the hexahedral meshes of the two rotor subdomains are connected by non-conformal interfaces in the solver.

The boundary conditions at the suction and discharge of the compressor are highly unsteady and therefore difficult to specify. To provide good boundary locations, the ports were extended to get good convergence of the flow and to reduce the numerical discrepancies arising from pressure pulses in the flow. The working gas was air with an equation of state defined by the ideal gas law for density. The suction receiver pressure was 1 bar absolute and the discharge receiver pressures were 2 bar and 3 bar absolute. The convergence criterion for all the equations was targeted at 1.0x10-3 and the

coefficient loops for every time step were set at 10. During the solution, the rms residuals for all the time steps were between 1.0x10-3 and 5.0x10-3 for the momentum equation and below 1.0x10-3 for the continuity and energy equations. The calculations were run until cyclic repetition of the flow and pressure characteristics was identified at the boundaries. Each case was calculated with both a Laminar and an SST k-Omega Turbulence model.

3.3. *Results and Discussion*

3.3.1. *Compression characteristics*

Fig. 11 shows the compression characteristic of cases **1**, **3** and **4** for one full cycle on fine grids with a discharge pressure of 2.0 bar. With uniform rotors the maximum pressure goes up to 2.5bar and with variable geometry rotors the maximum pressure goes up to 3.0bar. **Case 3,** with a variable rotor pitch, and **Case 4,** with a variable rotor profile, have a steeper rise in internal pressure than **Case 1** which has constant rotor geometry. The highest peak pressure is achieved with the variable pitch rotors. For a discharge pressure of 2.0bar this internal pressure rise is the result of over-compression.

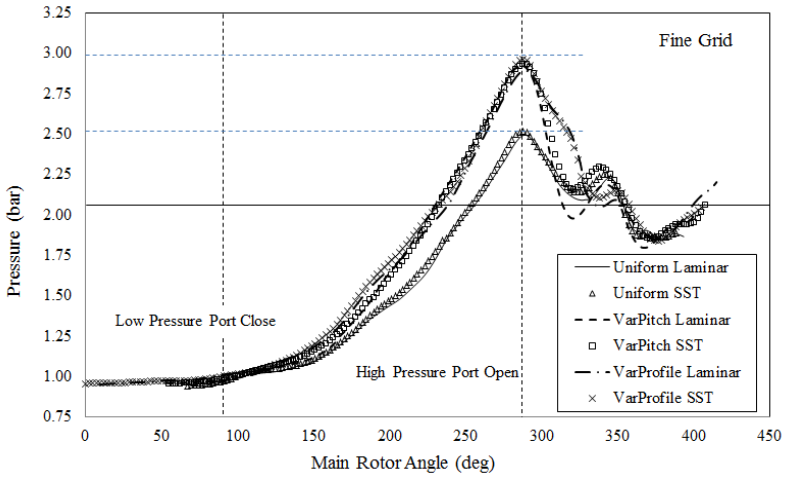

Fig. 11. Indicator diagram for Laminar and Turbulent cases with fine grid. Discharge pressure 2.0 bar

Fig. 12 shows the compression characteristic of the four cases on fine grids with discharge pressures of 2 bar and 3 bar and SST k-omega turbulence models. In the case of compression with uniform rotors, there is significant under compression at the point of opening of the discharge port, but with variable geometry rotors the maximum pressure goes up to 3.4bar

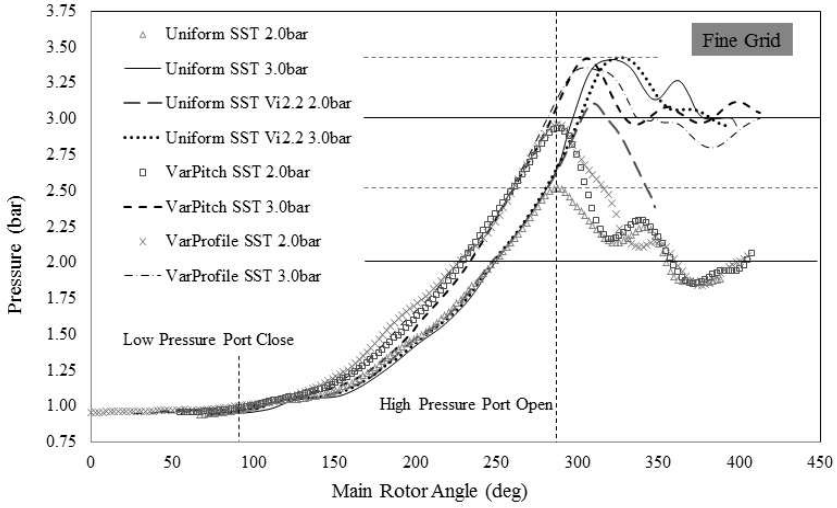

Fig. 12. Indicator diagram for cases calculated on fine grid with turbulence models. Discharge pressure 2.0bar and 3.0 bar

3.3.2. *Discharge Port Area*

Fig. 6 shows how the discharge port area decreases when the V_i is increased to 2.2. In **Case 2**, with uniform pitch and a reduced discharge port opening area, the internal pressure rises to about 3.1bar before exposure to a discharge pressure of 2 bar, as shown in Fig. 12 . This pressure rise was close to that with variable geometry rotors at about 3.0bar, for which the opening area was 22% higher. It should be noted that a larger discharge area for a comparable pressure rise reduces throttling losses in the compressor.

3.3.3. *Influence of grid refinement*

Fig. 13 shows the effect of grid refinement on the prediction of integral quantities such as the mass flow rate, indicated power and specific power for cases **1**, **3** and **4** with 2 bar discharge pressure. The mass flow rate showed an increase with grid refinement in all cases.

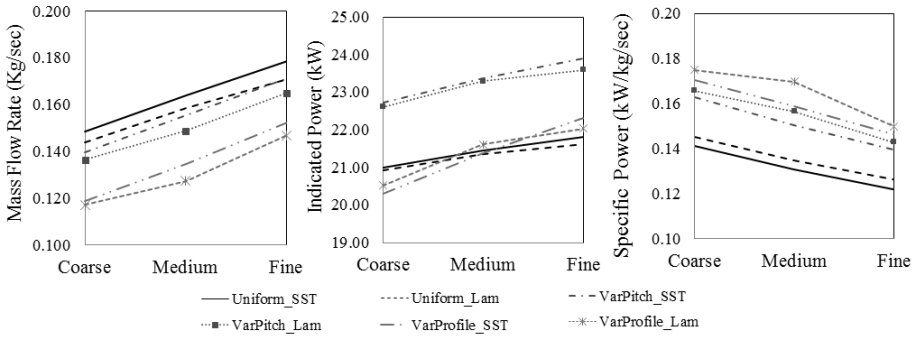

Fig. 13. Effect of grid refinement on integral parameters in cases 1,3 and 4 with 2.0bar discharge pressure

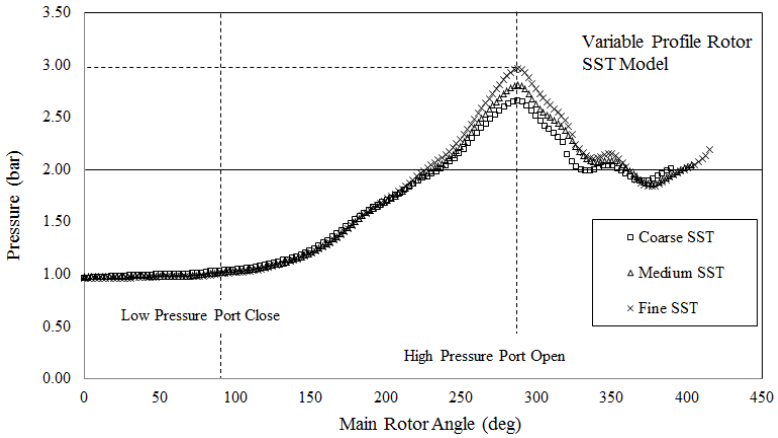

Fig. 14. Indicator diagram for cases 4 showing effect of grid refinement with 2.0bar discharge pressure

The difference between each consecutive grid refinement is around 10%. This is because the rotor geometry is captured better with finer grids, thereby resulting in reduced leakage. Similarly, the indicated power increases by 2-5% each time the grid is refined. The increase in the chamber pressure with grid refinement is shown in Fig. 14 for **Case 4,** with variable profile rotors as an example. In order to achieve a grid independent solution, it will be required to further refine the rotor domain grid in both the circumferential and axial directions.

3.3.4. *Influence of Turbulence Model*

As shown in Fig. 13, higher mass flow rates are achieved when the turbulence model is applied. The indicated power also increases as a consequence of the increased mass flow. However, the specific power is reduced for all turbulent cases indicating that the influence of turbulence models on mass flow rate prediction is higher than it is on indicator diagram/power prediction.

3.3.5. *Sealing Line Length*

The interlobe sealing line is the line of closest proximity between the two rotors. Leakage of gas takes place through this gap and is proportional to the length of the sealing line and the clearance normal to it [Fleming et. al, 1997, Hanjalic and Stosic, 1997]. Contours of pressure distribution on the rotors can be established and the dividing line between high and low pressure levels can be considered as the sealing line. The maximum pressure gradient is present across this division and is the driving force for leakage.Fig. 15 shows the sealing lines obtained on the uniform pitch rotors (**Case 1**) and variable geometry rotors (**Case 3** and **Case 4**). The projection of the sealing line on the rotor normal plane shows the difference more clearly. The sealing line on the uniform pitch rotor is of the same length for each interlobe space along the rotor. However, on the variable pitch rotors the sealing line is longer at the suction end but decreases towards the discharge end of the rotor.

Table 2 Comparison of Interlobe Sealing Line Length [mm]

Interlobe No	Uniform	Variable Pitch	Difference	Variable Profile	Difference
1	145.8	175.9	-30.1	158.4	-12.6
2	170.3	164.0	+6.4	162.2	+08.1
3 (part)	069.1	056.8	+12.2	068.4	+00.6
Total	385.2	396.6	-11.5	389.1	-03.9

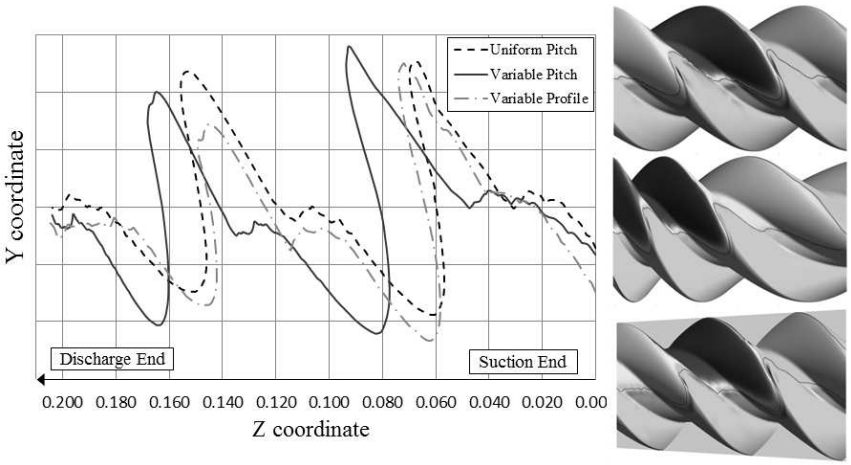

Fig. 15. Comparison of interlobe sealing line lengths

Table 2 presents the variation in the sealing line lengths between the uniform and variable geometry cases at one of the rotor positions indicating the magnitude of change along the rotors. At the suction end, the sealing line on the variable pitch rotor is 30mm longer but at the discharge end it is 12mm shorter than the sealing line for the constant pitch rotors. This helps to reduce leakage, because the largest pressure difference across the sealing line is at the discharge end. In total, length of the sealing line is reduced by 11mm in the variable pitch rotors. In **Case 4** with a variable profile the sealing line at the suction end is 12mm longer but is only slightly different to that of the uniform profile rotor at the discharge end. There is no overall gain in the reduction of sealing line length because the thickness of the gate lobe increases near the discharge end of the rotors.

3.3.6. *Blow-hole area*

The blow-hole area is the leakage area formed between the male and female rotors and the casing at the rotor cusp as shown in Fig. 16. The blow-hole area on the high pressure side has a significant effect on leakage due to the pressure difference between adjacent compression chambers. A smaller blow-hole area is desired for improved performance of the machine. Table 3 shows the blow-hole areas measured on the medium size grid for different calculated cases at three positions on the rotor. The blow-hole area for the uniform rotors remains constant along the length of the rotors. In the variable pitch rotors, the suction side blow-hole area is larger than in the uniform rotors but the discharge side

blow-hole area is smaller than for the uniform rotors. In the variable profile rotors, the suction side blow-hole area is nearly the same as that of the uniform rotors but the discharge blow-hole area is smaller than for the uniform rotors. Proportionally, the reduction of blow-hole area towards the discharge side rotors is most pronounced in the case of variable pitch rotors.

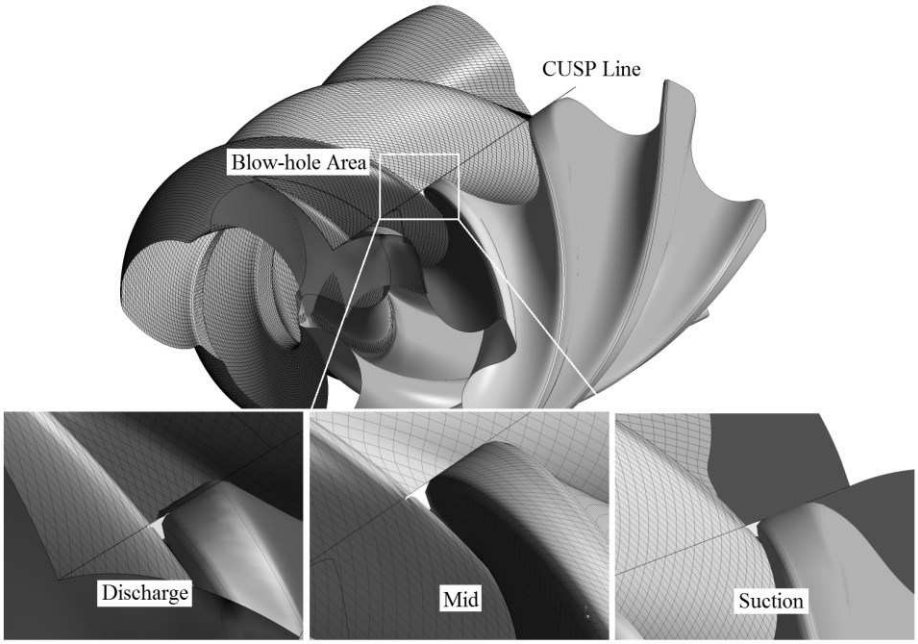

Fig. 16. Comparison of Blow-hole area

Table 3 Comparison of Blow-hole area [mm2]

Position	Uniform	Variable Pitch	Difference %	Variable Profile	Difference %
Suction	9.817	12.49	-27.2	9.83	-0.15
Mid	9.908	9.263	6.51	9.35	5.64
Discharge	9.701	6.562	32.3	9.19	5.29

3.3.7. *Overall performance*

For the analyzed cases **1**, **3** and **4,** the influence of the discharge pressure on compressor performance is shown in Fig. 17. Uniform rotors have the highest flow rate and the lowest specific power for both pressures. However the difference in the specific power between the uniform and the variable geometry rotors is much reduced at higher pressures. Table 4 shows a comparison of predicted volumetric and adiabatic efficiencies. Uniform rotors show the highest volumetric efficiency at 2 bar. But with a V_i of 2.2 the efficiency is lower than that of variable pitch rotors due to comparable internal pressure rise and comparatively shorter sealing line length in the variable pitch rotors. Also variable pitch rotors have a higher volumetric efficiency at a discharge pressure of 3 bar.

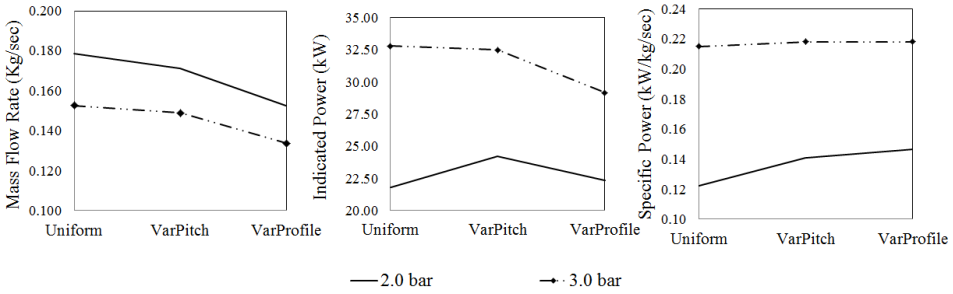

Fig. 17. Comparison of performance at 2.0bar and 3.0bar discharge pressure with fine grid cases

Table 4 Comparison of predicted variable geometry rotor efficiencies

	Built-in Volume Index	**Volumetric Efficiency %**		**Adiabatic Efficiency %**	
		2.0 bar	3.0 bar	2.0 bar	3.0 bar
Uniform	Vi 1.8	75.30	56.70	54.13	51.73
Uniform	Vi 2.2	64.00	55.66	44.06	49.91
Variable Pitch	Vi > 1.8	66.20	57.60	46.88	50.99
Variable Profile	Vi > 1.8	62.80	55.04	45.16	51.01

Uniform rotors show the highest adiabatic efficiency at 2 bar. But with a V_i of 2.2 the efficiency is lower than that of the variable geometry rotors. At 3 bar, variable geometry rotors with Vi=1.8 have an equal adiabatic efficiency to uniform rotors with the same Vi. This is due to reduced over-compression losses at 3 bar discharge pressure. This gives further indication that variable pitch rotors are more suitable for high pressure applications.

Variable profile rotors show a lower volumetric efficiency than uniform rotors due to the smaller capacity of the machine and also to the higher internal pressure rise. The over-compression before discharge results in a lower adiabatic efficiency except at 3 bar discharge pressure where it is comparable with uniform rotors.

3.4. *Conclusion*

A 3D grid generation procedure for twin screw compressors with variable pitch and variable profile rotors has been developed and used to carry out performance predictions for such machines using CFD. Examples of grids with variable geometries have been presented and analysis, using them, has shown the flow characteristics within these machines.

As a result, it has been shown that by varying the rotor lead continuously from the suction to the discharge ends, it is possible to achieve a steeper internal pressure build up. The analysis also showed that varying the rotor lead allows a larger size of discharge port

area, thereby reduced discharge losses, while providing increased volumetric efficiency by reducing the sealing line length in the high pressure zone. Analysis of variable profile rotors also showed a steeper internal pressure rise but there was no reduction in the sealing line length and blow-hole area with this type of rotors. The increase in root diameter of the female rotors with variable profile certainly helps in producing stiff rotors for high pressure applications.

These grid generation developments open new opportunities for further investigation of the flow behavior and improvements in the performance of these machines.

4. Nomenclature

L – Rotor Length
D – Male Rotor Outer Diameter
Φ_w – Male Rotor Wrap Angle
α – Male rotor rotation angle
$\Delta\alpha$ – Increment in Male rotor rotation angle
n – Cross section number
Z – Axial distance along the rotors
Δ_Z – Increment in Axial distance
z_1 – Number of lobes on the Male rotor
z_2 – Number of lobes on the Female rotor
p – Lead at a given axial position on rotor
p_s – Starting Lead
p_e – Ending Lead
Δt – Time Step Size
V_i – Built in Volume Index

References

ANSYS 13.0, User Guide and Help Manual, 2011.

Eiseman, P. R. [1992] "Control Point Grid Generation", *Computers & Mathematics with Applications*, **24**, No.5/6, pp57-67.

Ferziger, J. H. and Peric, M.[1996]*Computational Methods for Fluid Dynamics*, (Springer, Berlin, Germany),ISBN 978-3-540-42074-3.

Fleming, J. S., Tang, Y. and Cook, G.[1998]"The Twin Helical Screw Compressor, Part 1: Development, Applications and Competitive Position, Part 2: A Mathematical Model of the Working process", *Proc. Inst. Mech. Eng. Part C J. Mech. Eng. Sci.*, **212**, p369.

Gardner, J. W.[1969] US Patent No 3,424,373 – Variable Lead Compressor. Patented 1969.

Hanjalic, K. and Stosic, N.[1997]"Development and Optimization of Screw machines with a simulation Model – Part II: Thermodynamic Performance Simulation and Design Optimization". *ASME Transactions. Journal of Fluids Engineering*. **119**, p664.

Kim, J. H. and Thompson, J. F.[1990]"Three-Dimensional Adaptive Grid generation on a Composite-Block Grid", *AIAA Journal*, **28**, 3, pp470-477.

Kovacevic, A., Stosic, N. and Smith, I. K.[2000]"Grid Aspects of Screw Compressor Flow Calculations", *Proceedings of the ASME Advanced Energy Systems Division*, **40**, p83.

Kovacevic, A.[2002]"Three-Dimensional Numerical Analysis for Flow Prediction in Positive Displacement Screw Machines", Ph.D. Thesis, School of Engineering and Mathematical Sciences, City University London, UK.

Kovacevic, A., Stosic, N. and Smith, I. K. [2003]"3-D Numerical Analysis of Screw Compressor Performance", *Journal of Comp. Methods in Sciences and Engineering*, **3**, 2, pp259-284.

Kovacevic, A., Stosic, N. and Smith, I. K.[2004]"A numerical study of fluid–solid interaction in screw compressors". *International Journal of Computer Applications in Technology*. **21**, 4, pp148 – 158.

Kovacevic, A.[2005]"Boundary Adaptation in Grid Generation for CFD Analysis of Screw Compressors", *Int. J. Numer. Methods Eng*., **64**, 3, pp401-426.

Kovacevic, A., Stosic, N. and Smith, I. K.[2007]*Screw compressors - Three dimensional computational fluid dynamics and solid fluid interaction*, (Springer-Verlag Berlin Heidelberg New York), ISBN 3-540-36302-5.

Liseikin, V. D.[1998]"Algebraic Adaptation Based on Stretching Functions", *Russian Journal for Numerical and Analytical Mathematical Modeling*, **13**, 4, pp307-324.

Liseikin, V. D.[1999]*Grid Generation Methods*, (Springer-Verlag), ISBN 3-540-65686-3.

Prasad, B. G. [2004]"CFD for Positive Displacement Compressors", *Proc. Int. Compressor Conf. at Purdue*. pp1689.

Rane, S., Kovacevic, A., Stosic, N. and Kethidi, M. [2013]"Grid Deformation Strategies for CFD Analysis of Screw Compressors", *Int Journal of Refrigeration*, http://dx.doi.org /10.1016/j.ijrefrig.2013.04.008.

Rane, S., Kovacevic, A., Stosic, N. and Kethidi, M. [2013], "CFD grid generation and analysis of screw compressor with variable geometry rotors", *International conference on compressors and their systems*, London, C1390/139.

Samareh, A. J. and Smith, R. E. [1992]"A Practical Approach to Algebraic Grid Adaptation", *Computers & Mathematics with Applications*, **24**, 5/6, pp69-81.

Shih, T. I. P., Bailey, R. T., Ngoyen, H. L. and Roelke, R. J.[1991]"Algebraic Grid Generation For Complex Geometries", *Int. J. Numer. Meth. Fluids*, **13**, pp1-31.

Soni, B. K.[1992]"Grid Generation for Internal Flow Configurations", *Computers & Mathematics with Applications*, **24**, 5/6, pp191-201.

Stosic, N. [1998]"On Gearing of Helical Screw Compressor Rotors", *Journal of Mechanical Engineering Science*, **212**, p587.

Stosic, N., Smith, I. K. and Kovacevic, A. [2005] *Screw Compressors: Mathematical Modeling and Performance Calculation*, (Springer Verlag, Berlin), ISBN: 3-540-24275-9.

Thompson, J. F.[1984]"Grid Generation Techniques in Computational fluid Dynamics", *AIAA Journal*, **22**, 11, pp1505-1523.

Thompson, J. F., Soni, B.and Weatherill, N. P.[1999]*Handbook of Grid generation*, (CRC Press).

Voorde, V. J., Vierendeels, J. and Dick, E. [2004]"Development of a Laplacian-based mesh generator for ALE calculations in rotary volumetric pumps and compressors". *Computer Methods in Applied Mechanics and Engineering*, **193**, 39–41, pp4401-4415